J|A|C|S
COMMUNICATIONS

Published on Web 06/28/2002

Decoupling Optical and Potentiometric Band Gaps in π-Conjugated Materials

Kimihiro Susumu and Michael J. Therien*

Department of Chemistry, University of Pennsylvania
Philadelphia, Pennsylvania 19104-6323

Received March 18, 2002

Low optical band gap (E_{op}) organic materials figure prominently in a wealth of optoelectronic devices.[1−4] The prominent, low-energy electronic transitions characteristic of such materials typically correlate with the presence of HOMO and LUMO levels that are extensively destabilized and stabilized, respectively, relative to the corresponding energy levels of the conjugated building blocks of the organic oligomer or polymer. As such, these conjugated structures manifest modest potentiometrically determined HOMO−LUMO gaps (E_p; $E_{1/2}{}^{0/+} - E_{1/2}{}^{-/0}$) that correlate closely with E_{op}.

The measured E_p and E_{op} values of low optical band gap oligomers and polymers commonly follow a predictable dependence upon conjugation length;[1−10] augmented HOMO destabilization and LUMO stabilization track with increasing size of the conjugated oligomer, until cation radical (positive polaron) and anion radical (negative polaron) delocalization (diffusion) lengths limit further perturbation of $E_{1/2}{}^{0/+}$ and $E_{1/2}{}^{-/0}$, respectively. The magnitude of polaron diffusion lengths depends on the nature of the conjugated building block and rarely extends over spatial dimensions that exceed a handful of monomer units. Strategies to further reduce E_{op} values in low optical band gap materials once such delocalization limits have been reached have included conjugation expansion of the monomeric unit[2,4] and engineering charge resonance interactions in the polymer backbone through the alternation of donor and acceptor moieties. [9,11−15] While these approaches commonly augment desired polymer optoelectronic properties such as the polarizability, hyperpolarizability, and conductivity, it is crucial to note that redox instability is a common shortcoming of organic materials that possess low optical band gaps. In this report, we outline a strategy that enables engineering of conjugated oligomeric structures that possess highly delocalized singlet (S_1) excited states yet manifest apparent $E_{1/2}{}^{0/+}$ and $E_{1/2}{}^{-/0}$ values that are essentially invariant with respect to those elucidated for their constituent monomeric precursors.

Figure 1 displays exemplary conjugated (porphinato)metal oligomers[16] that feature a *meso*-to-*meso* ethyne-bridged linkage topology, along with their corresponding ethyne-elaborated (porphinato)zinc(II) (PZn) building blocks (**E-D**, **E$_2$-D**, **E$_2$-A**). This mode of macrocycle-to-macrocycle connectivity gives rise to extensive interpigment electronic interactions.[17−22] Compounds **E-D**, **E$_2$-D**, **DD**, **DDD**, and **DDDDD** constitute highly soluble analogues of previously studied examples of this structural motif having simple 10,20-diaryl substituents,[17−22] while **DA**, **DAD**, and **DADAD** define related conjugated arrays in which electron-rich and electron-poor PZn units alternate. Importantly, these **A** porphyrin units feature macrocycle 10,20-bis(perfluoroalkyl) groups. Potentiometric and electronic structural studies establish that [5,15-bis(perfluoroalkyl)-porphinato]zinc(II) species possess HOMOs and LUMOs that are uniformly lowered in energy by ∼0.3 eV relative to corresponding

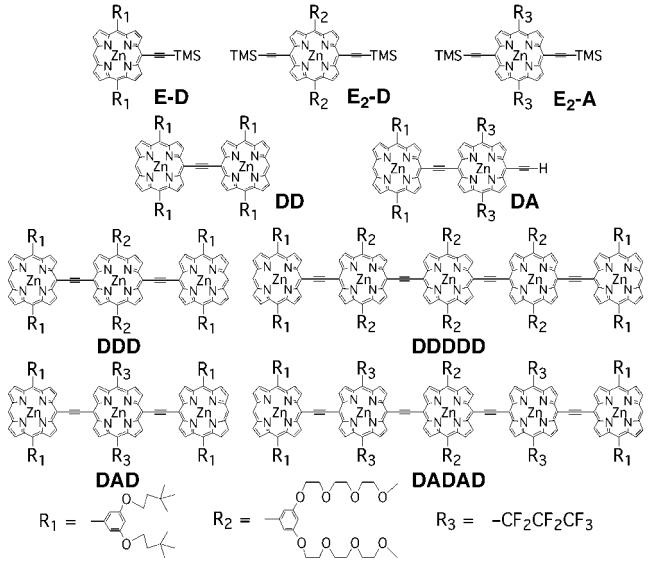

Figure 1. Structures of bis-, tris-, and pentakis[(porphinato)zinc(II)] compounds **DD**, **DA**, **DDD**, **DAD**, **DDDDD**, and **DADAD**, along with ethyne-elaborated (porphinato)zinc(II) building blocks **E-D**, **E$_2$-D**, and **E$_2$-A**.

meso-phenyl-substituted structures; furthermore, because the non-π-conjugating, σ-electron-withdrawing perfluoroalkyl group stabilizes extensively the PZn a_{2u} orbital, such species manifest a_{1u}-derived HOMOs.[23−25]

Figure 2 displays optical spectra for these classes of highly conjugated PZn arrays. Arrays **DD** and **DDD** display absorptive and emissive signatures similar to those elucidated for their parent compounds that bear unelaborated phenyl groups (Figure 1).[17] Impressively, conjugation length expansion of this motif utilizing a combination of PZn building blocks with 10- and 20-[3,5-bis(9-methoxy-1,4,7-trioxanonyl)phenyl] and [3,5-bis(3,3-dimethyl-1-butyloxy)phenyl] substituents gives rise to a highly soluble pentakis(PZn) structure (Figure 1). While the electronic structural characteristics of *meso*-to-*meso* ethyne-bridged porphyrin compounds have been discussed previously, it is worth noting that **DDDDD** displays a high oscillator strength Q-state-derived $\pi-\pi^*$ absorption ($\lambda_{max} = 842$ nm) with an extinction coefficient exceeding 225 000 M^{-1} cm^{-1} (Figure 2A). The corresponding optical spectra for the DA-based arrays are shown in Figure 2B. Note that while the DA-conjugated porphyrin arrays display (i) B-state domain spectral breadths that exceed that observed for their corresponding DD counterparts and (ii) high oscillator strength, low-energy Q-derived transitions, and corresponding S_1-S_0 fluorescence emission bands that are blue-shifted slightly with respect to the analogous transitions of conjugated porphyrin arrays composed of all electron-rich macrocycles (Figure 2A), these two classes of ethyne-linked porphyrinic oligomers manifest remarkably similar optical proper-

* To whom correspondence may be sent. E-mail: therien@a.chem.upenn.edu.

10.1021/ja0203925 CCC: $22.00

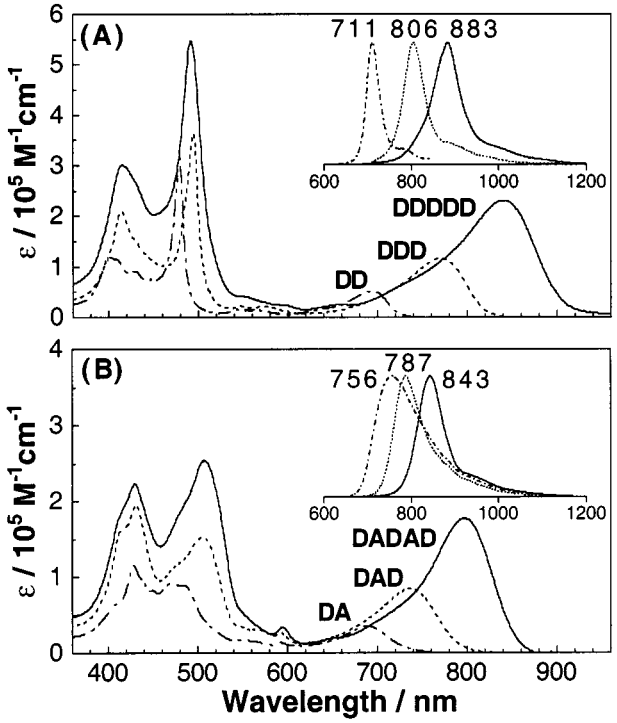

Figure 2. Room-temperature electronic absorption spectra of bis-, tris-, and pentakis[(porphinato)zinc(II)] arrays based on the DD and DA structural motifs in THF solvent: (A) **DD** (broken line), **DDD** (dotted line), and **DDDDD** (solid line); (B) **DA** (broken line), **DAD** (dotted line), and **DADAD** (solid line). Corrected emission spectra, with labeled emission wavelength maxima, are shown in the insets. Experimental details are available in the Supporting Information.

ties, displaying both the hallmarks of extensive π conjugation and exciton coupling.

Examination of the dependence of both E_p and E_{op} on increasing conjugation length, however, shows marked divergence between the conjugated DD and DA PZn arrays (Figure 3). The DD systems manifest (i) potentiometric responses indicating that the radical anion and radical cation states of these species become increasingly stabilized and destabilized, respectively, with increasing conjugation length and (ii) E(LUMO) − E(HOMO) potential differences (E_p's) that track with E_{op}; such characteristics epitomize the key properties of highly conjugated oligomers. In stark contrast, while optical data (Figure 2B) show that the DA oligomers manifest globally delocalized singlet-excited states, cyclic voltammetric data (Figure 3B) indicate that both the radical cation- and anion-state energy levels of these species vary little with increasing conjugation length. Note that the experimentally determined $E_{1/2}^{0/+}$ and $E_{1/2}^{-/0}$ potentials for these DA-conjugated oligomers resemble $E_{1/2}^{0/+}$ and $E_{1/2}^{-/0}$ values measured for benchmark ethyne-elaborated PZn monomers: Figure 3B underscores this uncommon redox behavior, highlighting that **DA**, **DAD**, and **DADAD** one-electron reduction potentials track the $E_{1/2}^{-/0}$ value established for **E$_2$-A**, while their corresponding one-electron oxidation potentials conform to the magnitude of $E_{1/2}^{0/+}$ determined for **E-D** (**E$_2$-D**).

Insight into this unusual electrooptic behavior can be gleaned from electronic structural analysis of the frontier orbitals (FOs) of the DD- and DA-conjugated oligomers. Figure 4 displays the HOMO−1, HOMO, LUMO, and LUMO+1 for the **DDD** and **DAD** supermolecular species. As expected,[21] the **DDD** HOMO exhibits substantial ethyne-, C_{meso}-, and N-centered electron density, with the C_{meso} carbons that constitute a portion of the conjugated macrocycle-to-macrocycle bridge displaying substantial π overlap with their respective C_α carbons; the **DDD** LUMO manifests

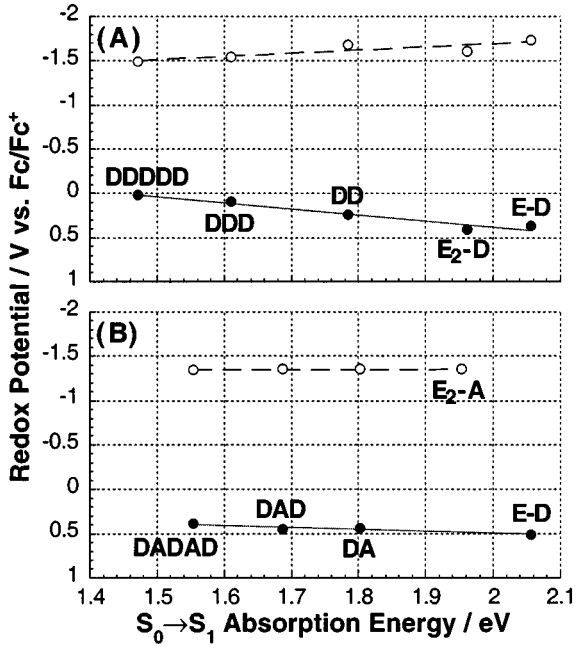

Figure 3. Dependence of the potentiometrically determined HOMO and LUMO energy levels upon the S_0-S_1 optical band gap (E_{op}) for (A) DD and (B) DA porphyrin arrays as a function of conjugation length. Oxidation and reduction potentials are denoted respectively by filled and open circles. All these redox potentials are relative to the ferrocene/ferrocenium (Fc/Fc^+) redox couple, which was used as an internal standard in these experiments. Solvent: for DD systems, CH_2Cl_2; for DA systems, THF. Tabulated potentiometric data are available in the Supporting Information.

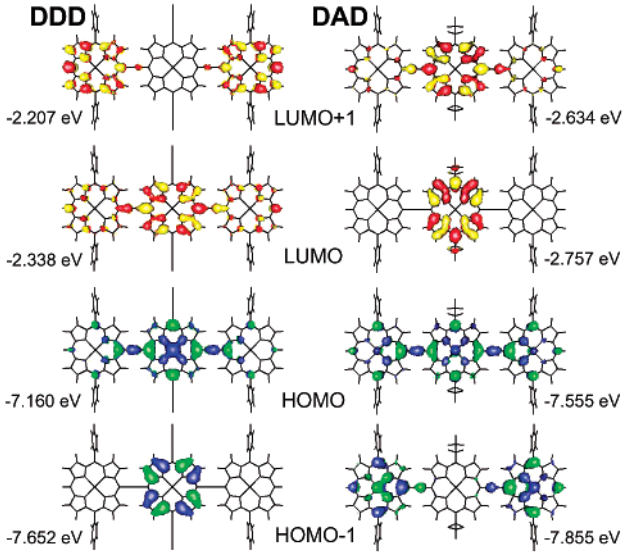

Figure 4. Frontier molecular orbitals for the tris[(porphinato)zinc(II)] species **DDD** and **DAD** determined from PM3 calculations. Computational details, as well as a more expansive set of frontier orbitals for these species, are available in the Supporting Information.

similarly comprehensive electronic delocalization, exhibiting extensive cumulenic character along the C_2 axis defined by the ethyne moieties.

The nature of the **DAD** FOs differ markedly from those elucidated for **DDD** (Figure 4); these differences derive from the fact that substantial energy gaps separate the **D**- and **A**-localized PZn fragment orbitals of equivalent symmetry (Supporting Information). Two effects of this are evident in the Figure 4 FOs. First, while the **DAD** HOMO bears an electron density distribution similar to that determined for the analogous **DDD** orbital, note that it lies

0.4 eV lower in energy; this energy difference is reflected in the magnitudes of the respective $E_{1/2}^{0/+}$ values determined for these species in the anodic electrochemistry. Two σ-electron-withdrawing perfluoroalkyl groups thus stabilize the FOs of *meso*-to-*meso* ethyne-bridged tris[P(Zn)] compounds to an extent similar to which these two substituents stabilize **A**-type PZn monomers relative to their *meso*-aryl counterparts (Supporting Information);[23−25] this substituent-derived electronic stabilization counterbalances the magnitude of HOMO destabilization that occurs concomitant with *meso*-to-*meso* ethynyl conjugation of three PZn monomer units in **DDD**. Second, in contrast to the case for **DDD**, note that the **DAD** LUMO is localized exclusively upon the central [10,20-bis-(perfluoroalkyl)porphinato]zinc(II) unit, with electron density distributed primarily upon the pyrrole C_α, C_β, and N atoms, and the *meso* carbon positions lying orthogonal to the highly conjugated supermolecular axis. Figure 4 hence underscores the cardinal role that **D** and **A** PZn fragment orbital energy differences play in fixing the potentiometrically determined, conjugation-length-independent radical cation- and anion-state energy levels evinced in Figure 3B for the DA PZn oligomers. It is important to appreciate that, in contrast to many simple conjugated organic building blocks, whose low-lying excited states are described adequately by one-electron transitions, extensive configuration interaction (CI) is necessary to describe correctly porphyrin electronically excited states.[26] While absolute HOMO and LUMO energies and electron density spatial distributions largely determine $E_{1/2}^{0/+} - E_{1/2}^{-/0}$ values, large CI guarantees orbital contributions from multiple high-lying filled and low-lying empty levels in DA PZn array excited states; consequently, globally delocalized S_1 states are realized.

In sum, we show that the magnitudes of the potentiometric HOMO−LUMO gap (E_p) and optical band gap (E_{op}) in conjugated organic materials can be modulated independently. For these ethyne-bridged porphyrin arrays, four factors appear crucial in achieving such optoelectronic characteristics: (i) conjugated building blocks that feature electronically excited states described by a multiconfigurational wave function; (ii) an alternating electron-rich/electron-poor structural motif, in which mismatched PZn fragment orbital energies attenuate severely radical anion delocalization between adjacent pigments along the highly conjugated oligomer axis; (iii) σ-electron-withdrawing macrocycle substituents that suppress effectively progressive HOMO level destabilization that occurs normally with increasing conjugation length; and (iv) strong electronic coupling between these conjugated units. Notably, because electrochemical responses obtained for DA porphyrin arrays resemble those elucidated for their monomeric building blocks, this work demonstrates that oxidative and reductive stability of highly conjugated polymers need not be sacrificed in order to achieve extensive excited-state electronic delocalization; the design strategy outlined herein may thus prove valuable in the evolution of new classes of redox-stable, low optical band gap processable organic optical materials.

Acknowledgment. This work was supported through the MRSEC Program of the National Science Foundation (DMR00-79909) and the Office of Naval Research (N00014-98-1-0725). M.J.T. and K.S. thank respectively the Camille and Henry Dreyfus Foundation and the Japanese Society for the Promotion of Science for research fellowships.

Supporting Information Available: Detailed syntheses and characterization data, tabulated optical and electrochemical data, along with the frontier molecular orbitals determined for the **DDD** and **DAD** arrays and a selection of benchmark (porphinato)zinc(II) species (PDF). This material is available free of charge via the Internet at http://pubs.acs.org.

References

(1) Tour, J. M. *Chem. Rev.* **1996**, *96*, 537−553.
(2) Roncali, J. *Chem. Rev.* **1997**, *97*, 173−205.
(3) Martin, R. E.; Diederich, F. *Angew. Chem., Int. Ed.* **1999**, *38*, 1350−1377.
(4) van Mullekom, H. A. M.; Vekemans, J. A. J. M.; Havinga, E. E.; Meijer, E. W. *Mater. Sci. Eng.* **2001**, *32*, 1−40.
(5) Bohnen, A.; Räder, H. J.; Müllen, K. *Synth. Met.* **1992**, *47*, 37−63.
(6) Kiehl, A.; Eberhardt, A.; Adam, M.; Enkelmann, V.; Müllen, K. *Angew. Chem., Int. Ed. Engl.* **1992**, *31*, 1588−1591.
(7) Meerholz, K.; Heinze, J. *Electrochim. Acta* **1996**, *41*, 1839−1854.
(8) Gebhardt, V.; Bacher, A.; Thelakkat, M.; Stalmach, U.; Meier, H.; Schmidt, H.-W.; Haarer, D. *Synth. Met.* **1997**, *90*, 123−126.
(9) van Mullekom, H. A. M.; Vekemans, J. A. J. M.; Meijer, E. W. *Chem. Eur. J.* **1998**, *4*, 1235−1243.
(10) Jestin, I.; Frére, P.; Mercier, N.; Levillain, E.; Stievenard, D.; Roncali, J. *J. Am. Chem. Soc.* **1998**, *120*, 8150−8158.
(11) Havinga, E. E.; ten Hoeve, W.; Wynberg, H. *Synth. Met.* **1993**, *55*−*57*, 299−306.
(12) Yamamoto, T.; Zhou, Z.-h.; Kanbara, T.; Shimura, M.; Kizu, K.; Maruyama, T.; Nakamura, Y.; Fukuda, T.; Lee, B.-L.; Ooba, N.; Tomaru, S.; Kurihara, T.; Kaino, T.; Kubota, K.; Sasaki, S. *J. Am. Chem. Soc.* **1996**, *118*, 10389−10399.
(13) Demanze, F.; Yassar, A.; Garnier, F. *Macromolecules* **1996**, *29*, 4267−4273.
(14) Zhang, Q. T.; Tour, J. M. *J. Am. Chem. Soc.* **1997**, *119*, 5065−5066.
(15) Yu, W.-L.; Meng, H.; Pei, J.; Huang, W. *J. Am. Chem. Soc.* **1998**, *120*, 11808−11809.
(16) For other examples of highly conjugated porphyrin oligomers, see: (a) Arnold, D. P.; Heath, G. A. *J. Am. Chem. Soc.* **1993**, *115*, 12197−12198. (b) Wytko, J.; Berl, V.; McLaughlin, M.; Tykwinski, R. R.; Schreiber, M.; Diederich, F.; Boudon, C.; Gisselbrecht, J.-P.; Gross, M. *Helv. Chim. Acta* **1998**, *81*, 1964−1977. (c) Taylor, P. N.; Huuskonen, J.; Rumbles, G.; Aplin, R. T.; Williams, E.; Anderson, H. L. *Chem. Commun.* **1999**, 909−910. (d) Tsuda, A.; Osuka, A. *Science* **2001**, *293*, 79−82.
(17) Lin, V. S.-Y.; DiMagno, S. G.; Therien, M. J. *Science* **1994**, *264*, 1105−1111.
(18) Lin, V. S.-Y.; Therien, M. J. *Chem. Eur. J.* **1995**, *1*, 645−651.
(19) Angiolillo, P. J.; Lin, V. S.-Y.; Vanderkooi, J. M.; Therien, M. J. *J. Am. Chem. Soc.* **1995**, *117*, 12514−12527.
(20) Kumble, R.; Palese, S.; Lin, V. S.-Y.; Therien, M. J.; Hochstrasser, R. M. *J. Am. Chem. Soc.* **1998**, *120*, 11489−11498.
(21) Shediac, R.; Gray, M. H. B.; Uyeda, H. T.; Johnson, R. C.; Hupp, J. T.; Angiolillo, P. J.; Therien, M. J. *J. Am. Chem. Soc.* **2000**, *122*, 7017−7033.
(22) (a) Fletcher, J. T.; Therien, M. J. *Inorg. Chem.* **2002**, *41*, 331−341. (b) Fletcher, J. T.; Therien, M. J. *J. Am. Chem. Soc.* **2002**, *124*, 4298−4311.
(23) DiMagno, S. G.; Williams, R. A.; Therien, M. J. *J. Org. Chem.* **1994**, *59*, 6943−6948.
(24) Goll, J. G.; Moore, K. T.; Ghosh, A.; Therien, M. J. *J. Am. Chem. Soc.* **1996**, *118*, 8344−8354.
(25) Moore, K. T.; Fletcher, J. T.; Therien, M. J. *J. Am. Chem. Soc.* **1999**, *121*, 5196−5209.
(26) Gouterman, M. In *The Porphyrins*; Dolphin, D., Ed.; Academic Press: London, 1978; Vol. III, pp 1−165.

JA0203925